

Magnetic anisotropies and magnetization reversal of the $\text{Co}_2\text{Cr}_{0.6}\text{Fe}_{0.4}\text{Al}$ Heusler compound

J. Hamrle,¹ S. Blomeier,¹ O. Gaier,¹ B. Hillebrands,¹ R. Schäfer,² and M. Jourdan³

¹*Fachbereich Physik and Forschungsschwerpunkt MINAS,*

Technische Universität Kaiserslautern,

Erwin-Schrödinger-Straße 56, D-67663 Kaiserslautern, Germany

²*IFW Dresden, Helmholtzstraße 20, D-01069 Dresden, Germany*

³*Institut für Physik, Johannes-Gutenberg-Universität,*

Staudinger Weg 7, D-55128, Mainz, Germany

(Dated: June 08, 2006)

Abstract

Magnetic anisotropies and magnetization reversal properties of the epitaxial Heusler compound $\text{Co}_2\text{Cr}_{0.6}\text{Fe}_{0.4}\text{Al}$ (CCFA) deposited on Fe and Cr buffer layers are studied. Both samples exhibit a growth-induced fourfold anisotropy, and magnetization reversal occurs through the formation of stripy domains or 90° domains. During rotational magnetometric scans the sample deposited on Cr exhibits about 2° sharp peaks in the angular dependence of the coercive field, which are oriented along the hard axis directions. These peaks are a consequence of the specific domain structure appearing in this particular measurement geometry. A corresponding feature in the sample deposited on Fe is not observed.

I. INTRODUCTION

Studies of ferromagnetic (FM) half-metals are mainly driven by their possible applications for spintronic devices as a potential source of a 100% polarized spin current. Some Heusler alloys are promising candidates due to their high Curie temperature and expected half-metallicity even for partially disordered systems.

Among the many Heusler systems already studied, the compound $\text{Co}_2\text{Cr}_{0.6}\text{Fe}_{0.4}\text{Al}$ (CCFA) attracted significant experimental^{1,2,3,4,5,6,7} and theoretical^{8,9,10} attention. CCFA is an interesting candidate due to its high Curie temperature of 760 K³ and its high value of volume magnetization of $\approx 3\mu_B$ per formula unit^{6,11} at 5 K (the theoretical value is $3.8\mu_B$ per formula unit¹²). At room temperature, CCFA exhibits a magnetoresistance of 30% for the pure Heusler compound in powder form¹³ or 88% if artificial Al_2O_3 grain boundaries⁷ are used. Simple $\text{Co}_2\text{Cr}_{0.4}\text{Fe}_{0.6}\text{Al}/\text{Cu}/\text{Co}_{90}\text{Fe}_{10}$ trilayers showed a large giant magnetoresistance of 6.8% at RT,⁴ while a tunneling magnetoresistance ratio of 52% at RT and 83% at 5K was reported for the system $\text{CCFA}/\text{AlO}_x/\text{Co}_{75}\text{Fe}_{25}$.¹¹

In this article we study magnetic anisotropies and magnetization reversal properties of epitaxial CCFA films deposited on Fe and Cr buffer layers.

II. SAMPLE PROPERTIES AND PREPARATION

We have investigated two samples consisting of CCFA sputtered onto an epitaxial Fe or Cr buffer layer: $\text{Al}(2.5\text{ nm})/\text{CCFA}(80\text{ nm})/\text{Cr}(8\text{ nm})/\text{MgO}(001)$ (in the following called CCFA/Cr) and $\text{Al}(4\text{ nm})/\text{CCFA}(105\text{ nm})/\text{Fe}(10\text{ nm})/\text{MgO}(001)$ (in the following called CCFA/Fe). The buffer layers were deposited by electron beam evaporation onto a single-crystalline $\text{MgO}(001)$ substrate, while the epitaxial CCFA films were subsequently deposited by dc magnetron sputtering. A more detailed description of the sample preparation procedure can be found elsewhere.⁶ The films grow with the B2 structure, as there is full disorder between the Cr and Al positions, but order on the Co positions.⁶ A volume magnetization of $\mu_{\text{CCFA}} \approx 2.5\mu_B$ per formula unit was measured at 300 K.⁶ 4-circle XRD scans yielded axes lengths of $a = 0.569 \pm 0.003\text{ nm}$, $b = c = 0.578 \pm 0.006\text{ nm}$ ($a = 0.570 \pm 0.005\text{ nm}$, $b = c = 0.583 \pm 0.012\text{ nm}$) for CCFA/Fe (CCFA/Cr), where the a -axis is perpendicular to the sample surface and b and c are in-plane axes. Therefore, in-plane strain is as small as

$\approx 0.8 \pm 2.6\%$.

III. MAGNETIC ANISOTROPIES

Magnetic anisotropies were investigated using magneto-optical Kerr effect (MOKE) magnetometry. All measurements were performed in longitudinal geometry with an angle of incidence near 45° . The MOKE hysteresis loops were measured as a function of the in-plane angle α of the applied magnetic field with respect to the in-plane $[100]$ direction of the CCFA film by rotating the sample about its normal axis and recording the loop every 1° . Typical loops as well as the corresponding polar plots of the obtained coercivity for CCFA/Cr and CCFA/Fe are presented in Figs. 1 and 2. In both figures, the $[100]$ CCFA axis (i.e. the $[110]$ axis of the MgO substrate⁶) corresponds to a sample orientation of $\alpha = 0^\circ$. As it can be seen in the figure, both the CCFA/Cr and CCFA/Fe samples show a fourfold in-plane anisotropy reflecting the crystallographic symmetry of the CCFA film. Several interesting features can be observed:

(1) The maximum coercivities for CCFA/Fe and CCFA/Cr are 28 and 29 Oe, respectively, and are thus very similar.

(2) The in-plane easy axes lie along the $\langle 100 \rangle$ CCFA axes for CCFA/Fe whereas in case of CCFA/Cr they are rotated by 45° , i.e. oriented along the $\langle 110 \rangle$ CCFA axes. At the moment, the reasons for this behavior are not clear. According to previous studies, both types of film grow with the same crystallographic orientation and thus should exhibit the same orientation of their magnetic easy axes.¹⁴

(3) CCFA/Cr exhibits unique sharp peaks in H_c as a function of the in-plane angle α as narrow as 2° . These peaks are aligned parallel to the $\langle 100 \rangle$ CCFA hard axes. As it will be shown in the next section, they originate from a peculiar magnetization reversal mechanism when H is applied exactly parallel to the $\langle 100 \rangle$ CCFA hard axis. Similar peaks have been observed on epitaxial bcc Fe on Cu(001):¹⁵ in this case the origin of the peaks was attributed to the presence of structural microdomains in Fe, having different easy and hard axes and being magnetically coupled to each other. However, as it will be discussed later, in our case of CCFA/Cr the peaks originate from magnetic frustration effects during magnetization reversal.

IV. MAGNETIZATION REVERSAL

Magnetization reversal mechanisms were studied using a Kerr microscopy setup described in Ref.¹⁶. Using different orientations of a nearly crossed polarizer and analyzer we are sensitive to magnetization components both parallel and transverse to the externally applied field H . When the orientations of the analyzer and the polarizer are almost equal to 0° and 90° , the Kerr microscope is sensitive to the longitudinal magnetization component (i.e. the component parallel to the incidence plane of light). On the other hand, when the orientations of the analyzer and the polarizer are nearly equal to 45° and -45° , the microscope is sensitive to the transverse magnetization component (i.e. the component transverse to the plane of incidence).

The demagnetized state of CCFA/Cr is displayed in Fig. 3. The images shown in panels (a) and (b) are Kerr images of an identical domain structure, but with sensitivity to the magnetization components transverse and parallel to H , respectively. The sample was demagnetized by an AC field (frequency ≈ 10 Hz, maximal amplitude ≈ 80 Oe) applied in hard axis direction ($\alpha = 0^\circ$) whose amplitude was gradually decreased to zero. Both (a) and (b) Kerr images show a stripy domain pattern, with the stripe directions being parallel to the respective direction of the measured magnetization components. Therefore, the demagnetized state exhibits a 90° domain structure, as it is sketched in panel (c). The dots in the Kerr images are small particles on the sample surface, which do not influence domain propagation or nucleation. The demagnetized state of CCFA/Fe is very similar to that of CCFA/Cr (it also exhibits a 90° domain structure), so we do not discuss it here any further.

We now address the origin of the peaks in the coercivity of CCFA/Cr. Figure 4(a) shows a Kerr image of CCFA/Cr at an angle of $\alpha \approx 3^\circ$ (i.e. in an 'out-of-peak' orientation), after the sample had been saturated in a negative field and a field of 21 Oe had subsequently been applied. The image was recorded with sensitivity to the magnetization component parallel to the direction of the applied magnetic field. For the in-plane transverse magnetization component we did not get any contrast, i.e. this magnetization component is homogeneous. Hence, magnetization reversal solely happens by the appearance of a stripy domain structure, as it is sketched in Fig. 4(b). The magnetization within different domains points in different easy axis directions in such a way that the stripy domains are separated by 90° domain walls.

Figure 5(a) shows the reversal mechanism of CCFA/Cr when H is applied along the $\langle 100 \rangle$ CCFA hard axes direction ($\alpha = 0^\circ$). The sample had been saturated in a negative field and then the image was taken at a field value of 18 Oe, i.e. before the jump in the hysteresis loop appears. It should be noted that at this field value no contrast was found for the magnetization component parallel to H . Therefore, the domain configuration consist of stripes [sketched in Fig. 5(b)], which are again separated by 90° domain walls, but now the stripe direction is *transverse* to H . The observed stripy domain structure originates from a magnetic frustration effect, i.e. upon reduction of the external field the magnetization wants to rotate into the direction of an easy axis, but has to choose between two of these axes which are energetically equivalent. Therefore the magnetization splits into domains corresponding to these axes, as sketched in Fig. 5(b). If the external field is now further reduced, a jump in the respective hysteresis loop occurs, which is caused by the appearance of a 90° domain structure, as it is sketched in Fig. 6 (a). Thereafter, the magnetization again assumes a stripy domain configuration with a stripe direction transverse to H . The reversal mechanisms in both the 'peak' ($\alpha = 0^\circ$) and the 'out-of-peak' orientation ($\alpha \approx 3^\circ$) are schematically illustrated in Fig. 6.

During hard axis magnetization reversal of CCFA/Fe, no stripy domains transverse to the applied field H were observed, i.e. the only stripy domains observed were oriented parallel to H . Therefore, this magnetization reversal process is similar to the 'out-of-peak' reversal of CCFA/Cr sketched in Fig. 6(b).

Figure 7 displays snapshots of the magnetization reversal process of CCFA/Cr in easy axis direction ($\alpha = 45^\circ$). Panels (a) and (b) correspond to magnetization components transverse or parallel to the applied magnetic field, respectively. Magnetic domains are now mostly separated by 180° domain walls. However, in this case transverse spike domains containing a non-vanishing transverse magnetization component appear (highlighted by white circles in Fig. 7). In the case of CCFA/Fe, such domains are not observed.

V. SUMMARY

The magnetic properties of $\text{Co}_2\text{Cr}_{0.6}\text{Fe}_{0.4}\text{Al}$ (CCFA) films deposited onto Fe and Cr buffer layers were studied. Both films exhibit a fourfold magnetic anisotropy as well as a 90° domain structure with 90° domain walls in their demagnetized state. Magnetization reversal occurs

through the formation of different stripy domain or 90° domain structures. Furthermore, CCFA/Cr exhibits sharp peaks in H_c if H is applied parallel to the $\langle 100 \rangle$ CCFA hard axes directions. These peaks are related to the appearance of peculiar domain structures during reversal originating from a magnetic frustration effect. In the case of CCFA/Fe, such effects are not observed.

VI. ACKNOWLEDGEMENT

The project was financially supported by the Research Unit 559 "*New materials with high spin polarization*" funded by the Deutsche Forschungsgemeinschaft, and by the Stiftung Rheinland-Pfalz für Innovation. We would like to thank C. Hamann for help with the Kerr microscopy measurements and T. Mewes for stimulating discussions.

-
- ¹ H. J. Elmers, G. H. Fecher, D. Valdaitsev, S. A. Nepijko, A. Gloskovskii, G. Jakob, G. Schön-
hense, S. Wurmehl, T. Block, C. Felser, P.-C. Hsu, W.-L. Tsai, and S. Cramm, Phys. Rev. B
67, 104412 (2003).
- ² N. Auth, G. Jakob, T. Block, and C. Felser, Phys. Rev. B **68**, 024403 (2003).
- ³ C. Felser, B. Heitkamp, F. Kronast, D. Schmitz, S. Cramm, H. A. Dürr, H. Elmers, G. H. Fecher,
S. Wurmehl, T. Block, D. Valdaitsev, S. A. Nepijko, A. Gloskovskii, G. Jakob, G. Schönhense,
and W. Eberhardt, J. Phys. Condens. Matter **15**, 7019 (2003).
- ⁴ R. Kelekar and B. M. Clemens, Appl. Phys. Lett. **86**, 232501 (2005).
- ⁵ A. Hirohata, H. Kurebayashi, S. Okamura, N. Tezuka, and K. Inomata, IEEE Trans. Mag. **41**,
2802 (2005).
- ⁶ A. Conca, M. Jourdan, C. Herbort, and H. Adrian, cond-mat/0605698 (2006).
- ⁷ T. Block, S. Wurmehl, , C. Felser, and J. Windeln, Appl. Phys. Lett. **88**, 202504 (2006).
- ⁸ Y. Miura, K. Nagao, and M. Shirai, Phys. Rev. B **69**, 144413 (2004).
- ⁹ V. N. Antonov, H. A. Durr, Y. Kucherenko, L. V. Bekenov, and A. N. Yaresko, Phys. Rev. B
72, 054441 (2005).
- ¹⁰ S. Wurmehl, G. H. Fecher, K. Kroth, F. Kronast, H. A. Dürr, Y. Takeda, Y. Saitoh, K.
Kobayashi, H.-J. Lin, G. Schönhense, and C. Felser, J. Phys. D: Appl. Phys. **39**, 803 (2006).
- ¹¹ K. Inomata, S. Okamura, A. Miyazaki, M. Kikuchi, N. Tezuka, M. Wojcik, and E. Jedryka, J.
Phys. D: Appl. Phys. **39**, 816 (2006).
- ¹² I. Galanakis, J. Phys. Condens. Matter **14**, 6329 (2002).
- ¹³ T. Block, C. Felser, G. Jakob, J. Ensling, B. Mühling, P. Gütlich, and R. J. Cavac, J. Solid
State Chem. **176**, 646 (2003).
- ¹⁴ J. E. Mattson, E. E. Fullerton, C. H. Sowers, and S. D. Bader, J. Vac. Sci. Technol. A **13**, 276
(1995).
- ¹⁵ F. Scheurer, R. Allenspach, P. Xhonneux, and E. Courtens, Phys. Rev. B **48**, 9890 (1993).
- ¹⁶ A. Hubert and R. Schäfer, *Magnetic Domains: The Analysis of Magnetic Microstructures*
(Springer-Verlag, Berlin, 1998).

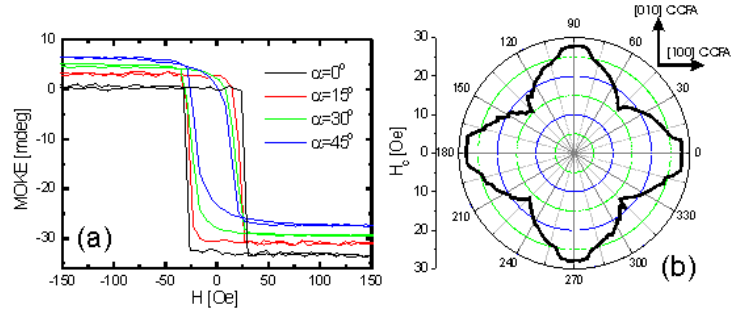


FIG. 1: (a) (color on-line) MOKE loops of CCFA/Fe for different sample orientations. (b) polar plot of the coercivity H_c .

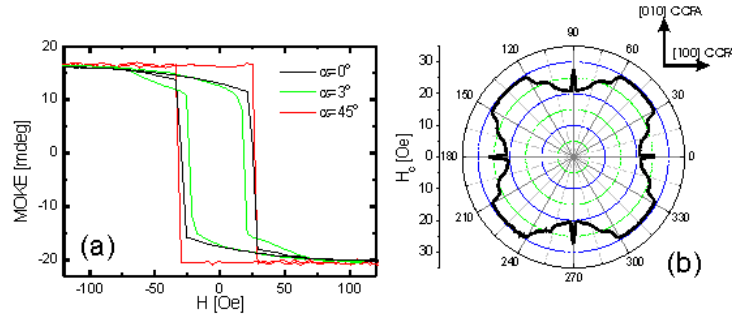


FIG. 2: (a) (color on-line) MOKE loops of CCFA/Cr for different sample orientations. (b) polar plot of the coercivity H_c .

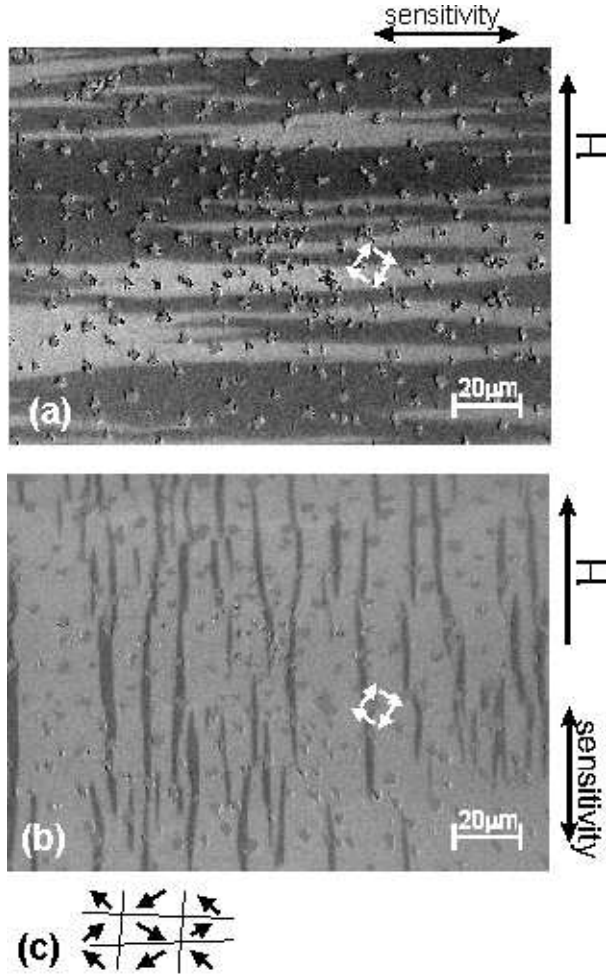


FIG. 3: Kerr microscopy image of the demagnetized state of CCFA/Cr. The demagnetizing AC field was applied in hard axis direction ($\alpha = 0^\circ$). The image corresponds to sensitivity to magnetization components (a) transverse and (b) parallel to H , respectively. Both images show an identical domain pattern, recorded under different sensitivity conditions. Magnetization directions are indicated by small white arrows. (c) Sketch of the underlying 90° domain structure.

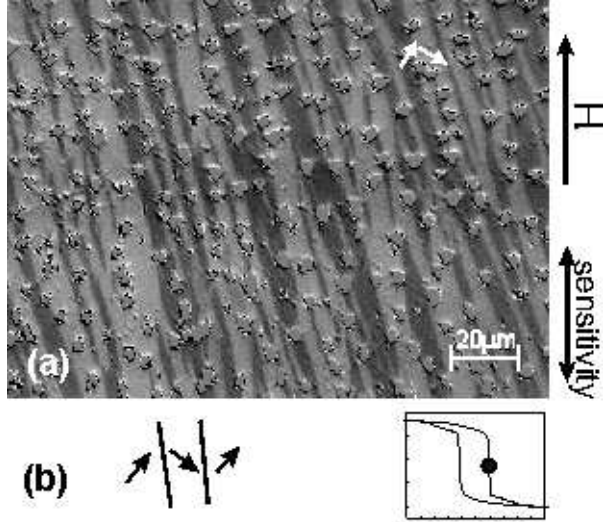


FIG. 4: Kerr microscopy image of CCFA/Cr at $H=21$ Oe at a sample orientation of $\alpha \approx 3^\circ$ ('out-of-peak' orientation). The image contrast corresponds to the magnetization component parallel to H . Magnetization directions are indicated by small white arrows. (b) Sketch of the observed stripy domain structure.

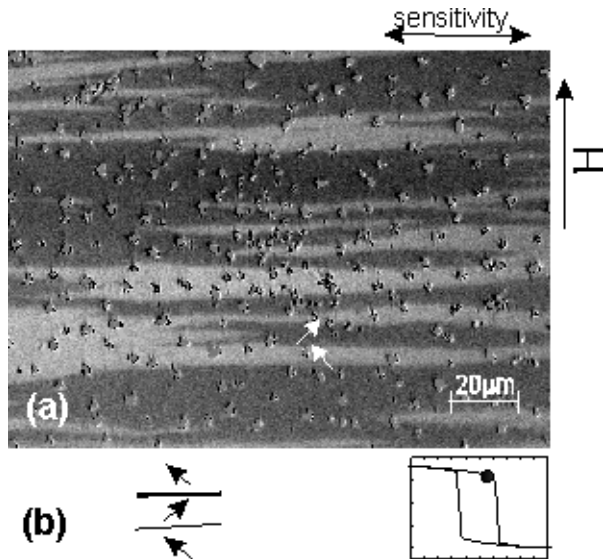


FIG. 5: Kerr microscopy image of CCFA/Cr at $H=18$ Oe at a sample orientation of $\alpha = 0^\circ$ ('peak' orientation). The image contrast corresponds to the magnetization component transverse to H . Magnetization directions are indicated by small white arrows. (b) Sketch of the stripy domain structure.

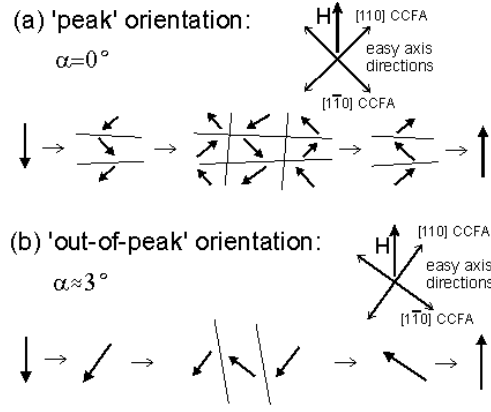


FIG. 6: Sketch of the magnetization reversal when (a) H is parallel to the $\langle 100 \rangle$ CCFA direction ('peak' orientation) and (b) when H is slightly deviated from the $\langle 100 \rangle$ CCFA direction ('out-of-peak' orientation).

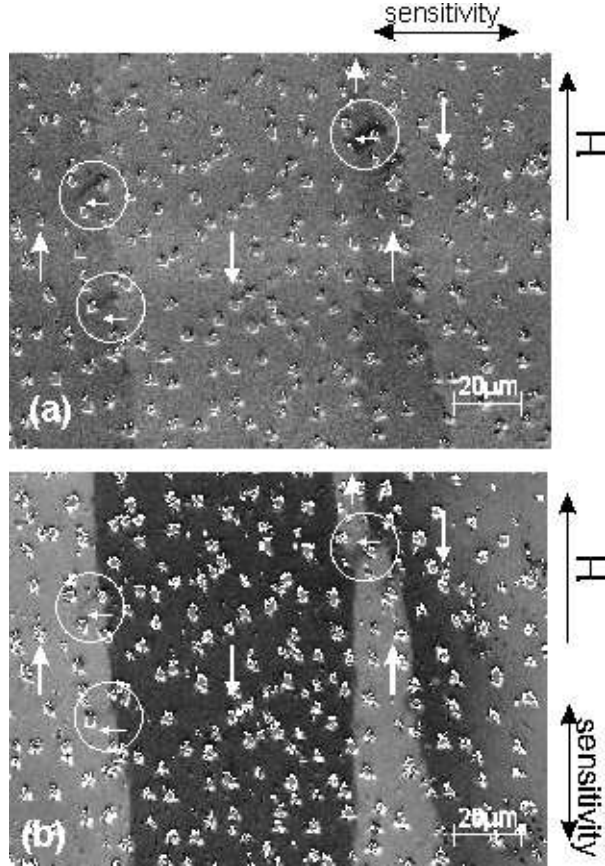


FIG. 7: Kerr microscopy images of CCFA/Cr at $H=29$ Oe corresponding to magnetization components (a) transverse and (b) parallel to H applied along the $[110]$ CCFA easy axis direction ($\alpha = 45^\circ$). Magnetization directions are indicated by small white arrows. Transversal spike domains are highlighted by white circles.